JOC Article

Guest Binding and New Self-Assembly of Bisporphyrins

Takeharu Haino,* Takashi Fujii, and Yoshimasa Fukazawa*

Department of Chemistry, Graduate School of Science, Hiroshima University, 1-3-1 Kagamiyama, Higashi-Hiroshima 739-8526, Japan

haino@sci.hiroshima-u.ac.jp; fukazawa@sci.hiroshima-u.ac.jp

Received October 26, 2005

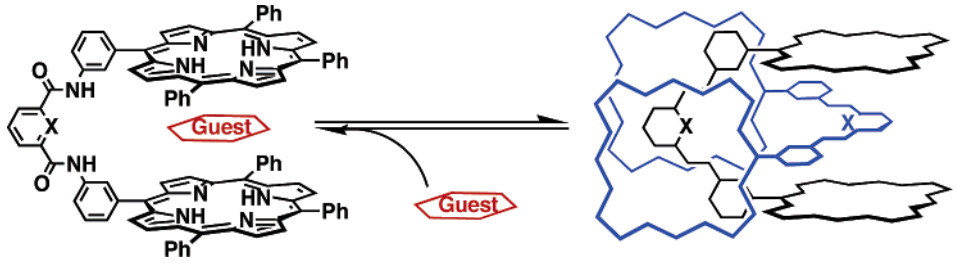

In organic medium, bisprophyrins **1**−**6** connected by aromatic linkers self-assemble via subtle forces such as van der Waals, $\pi-\pi$ stacking, and CH/π to form supramolecular dimers. The structures of bisporphyrin dimer **1·1** were discussed using our chemical shift simulation, revealing that **1·1** mainly adopts the self-complementary structure **A**. ESI mass experiments of the bisporphyrins showed that **1**−**4** form only the dimers; however, trimers as well as the dimers of **5** and **6** were observed in the gas phase. Thus, the assemblies of bisporphyrin **5** and **6** should adopt structure **B**, which still has a binding site to which another bisporphyrin can fit to form oligomeric structures. The dimerization constant of bisporphyrin **1** is dependent on the solvent polarity: the values decrease in the order of toluene > chloroform > 20% methanol−chloroform. The thermodynamic studies of the dimerization processes revealed that desolvation as well as $\pi-\pi$ stacking interactions play a key role in the formation of the self-complementary dimers. The binding studies of bisporphyrin **1** with a variety of electron deficient aromatic guests **9**−**17** were carried out in chloroform. Soret and Q-bands of **1** showed the characteristic changes with the addition of guests **9**−**13** and **15**, and large upfield shifts of their protons were observed in their complexation studies with ^{1}H NMR spectroscopy. These results suggested that the electron deficient aromatic guests bound within the cleft of bisporphyrin **1** via charge transfer as well as $\pi-\pi$ stacking interactions between the guests and the porphyrin rings. The dimerization constant of **1·1** is much smaller than the association constant of **1·9**, suggesting that the dissociation of dimer **1·1** can be regulated by binding of **9** within the cleft. The addition of **9** into the solution of **1·1** resulted in the quick dissociation of the dimer and the formation of **1·9**.

Introduction

Porphyrin is one of the most promising platforms for the construction of large molecular architectures. Numerous syntheses of porphyrin derivatives have been reported with unique functions. Above all, huge multiporphyrin architectures are the most challenging targets on the subject of mimicking the bacterial photosynthetic reaction center, light-harvesting antenna complexes, and electron-transfer processes in protein possessing heme groups. In fact, various artificial systems based on multiporphyrins have been designed and synthesized, which show photoinduced molecular switches, fluorescence sensors, photonic wires, and molecular elements for information storage.[1] Nanometric multiporphyrin arrays arising from the covalent

* Author to whom correspondence should be addressed. Phone: +81-82-424-7403. Fax: +81-82-424-0724.

(1) (a) Flamigni, L.; Talarico, A. M.; Serroni, S.; Puntoriero, F.; Gunter, M. J.; Johnston, M. R.; Jeynes, T. P. *Chem. Eur. J.* **2003**, *9*, 2649−2659. (b) Shinkai, S.; Ikeda, M.; Sugasaki, A.; Takeuchi, M. *Acc. Chem. Res.* **2001**, *34* (6), 494−503. (c) Guo, Y. M.; Oike, H.; Aida, T. *J. Am. Chem. Soc.* **2004**, *126*, 716−717. (d) Fujita, N.; Biradha, K.; Fujita, M.; Sakamoto, S.; Yamaguchi, K. *Angew. Chem., Int. Ed.* **2001**, *40*, 1718−1721. (e) Kim, D.; Osuka, A. *Acc. Chem. Res.* **2004**, *37*, 735−745. (f) Kim, D.; Osuka, A. *J. Phys. Chem. A* **2003**, *107*, 8791−8816. (g) Cho, H. S.; Jeong, D. H.; Cho, S.; Kim, D.; Matsuzaki, Y.; Tanaka, K.; Tsuda, A.; Osuka, A. *J. Am. Chem. Soc.* **2002**, *124*, 14642−14654. (h) Purrello, R.; Gurrieri, S.; Lauceri, R. *Coord. Chem. Rev.* **1999**, *190*−*192*, 683−706.

10.1021/jo052224b CCC: $33.50
Published on Web 03/10/2006

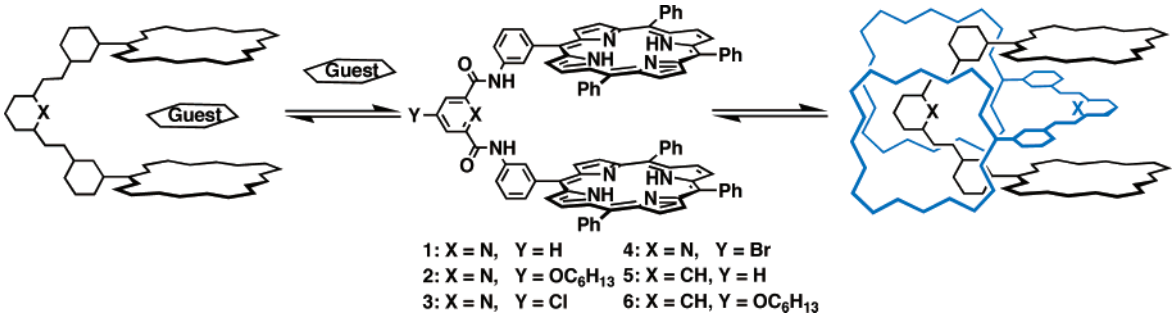

FIGURE 1. Schematic representation of dimeric and host−guest complexes of bisporphyrins.

synthesis have been reported.[2] However, conventional synthetic strategies to access multiporphyrin structures take multistep synthesis. In contrast, noncovalent synthesis based on self-assembly has emerged as a versatile alternative to covalent synthesis, and offers the easy and quick construction of huge multiporphyrin architectures. Metal coordination and hydrogen bonding are the most useful interactions for self-assembly. Numerous examples of multiporphyrin architectures via self-assembly through these interactions have been reported so far.[3]

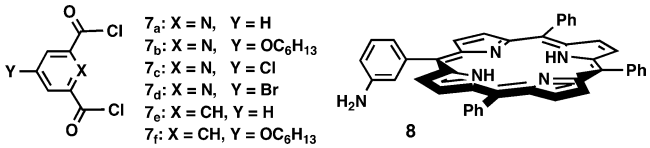

FIGURE 2. Building blocks for the bisporphyrin synthesis.

On the other hand, examples for self-assemblies of porphyrins due to the subtle forces such as van der Waals and CH/π interactions in organic medium are limited although porphyrin provides a flat, wide, and electron-rich surface, creating van der Waals, $\pi-\pi$ stacking, charge-transfer interactions, which play a significant role for self-assemblies.[4]

We have found that simple bisporphyrins connected by aromatic spacers showed self-dimerizations to form self-complementary structures via weak noncovalent interactions in organic solvent.[5] In this paper we report a full account of the self-dimerization behaviors and their properties for the recognition of aromatic guests within the clefts.

Results and Discussion

Bisporphyrins **1**−**6** were prepared by simple acylations of diacid chlorides $\mathbf{7_{a-f}}$[6] and porphyrin **8**.[7] Their ^{1}H NMR spectra were concentration dependent in chloroform. As the concentrations of **1** were increased, protons H_1, H_2, H_3, and H_4 were shifted upfield. Particularly, two broad multiplets of H_3 and H_4 appeared at 4.25 and 5.14 ppm at the concentration of 15.2 mmol/L. These unusual upfield shifts of the pyridyl protons place them in the strong shielding region of the porphyrin rings, forming supramolecular assemblies. Electrospray ionization (ESI) techniques have become a versatile tool to study a wide range of chemical and biological species.[8] The ESI mass measurements of the bisporphyrins gave an important insight into the structures of the assemblies formed. The ESI mass measurement of bisporphyrin **1** taken in positive mode revealed the intense peaks at *m*/*z* 2782 and 1391 attributable to $[\mathbf{1}\cdot\mathbf{1} + H]^+$ and $[\mathbf{1}\cdot\mathbf{1} + 2H]^{2+}$. The measured isotopic pattern for $[1 + H]^+$ and $[\mathbf{1}\cdot\mathbf{1} + 2H]^{2+}$ matched the calculated abundance,

(2) (a) Nishino, N.; Wagner, R. W.; Lindsey, J. S. *J. Org. Chem.* **1996**, *61*, 7534−7544. (b) Wagner, R. W.; Johnson, T. E.; Lindsey, J. S. *J. Am. Chem. Soc.* **1996**, *118*, 11166−11180. (c) Taylor, P. N.; Huuskonen, J.; Rumbles, G.; Aplin, R. T.; Williams, E.; Anderson, H. L. *Chem. Commun.* **1998**, 909−910. (d) Anderson, H. L. *Chem. Commun.* **1999**, 2323−2330. (e) Wytko, J.; Berl, V.; McLaughlin, M.; Tykwinski, R. R.; Schreiber, M.; Diederich, F.; Boundon, C.; Gisselbrecht, J.-P.; Gross, M. *Helv. Chim. Acta* **1998**, *81*, 1964−1977. (f) Mak, C. C.; Bampos, N.; Sanders, J. K. M. *Angew. Chem., Int. Ed.* **1998**, *37*, 3020−3023. (g) Mak, C. C.; Pomeranc, D.; Montalti, M.; Prodi, L.; Sanders, J. K. M. *Chem. Commun.* **1999**, 1083−1084. (h) Nakamura, Y.; Aratani, N.; Osuka, A.; Hwang, I.-W.; Ahn, T. K.; Ko, D. M.; Kim, D.; Takagi, A.; Kawai, T.; Matsumoto, T. *J. Am. Chem. Soc.* **2005**, *127*, 236−246. (i) Peng, X.; Aratani, N.; Osuka, A.; Takagi, A.; Matsumoto, T.; Kawai, T.; Hwang, I.-W.; Ahn, T. K.; Kim, D. *J. Am. Chem. Soc.* **2004**, *126*, 4468−4469. (j) Aratani, N.; Osuka, A.; Takagi, A.; Yanagawa, Y.; Matsumoto, T.; Kawai, T.; Yoon, Z. S.; Kim, D. *Chem. Eur. J.* **2005**, *11*, 3389−3404. (k) Takagi, A.; Yanagawa, Y.; Matsumoto, T.; Kawai, T.; Tsuda, A.; Aratani, N.; Osuka, A. *Chem. Commun.* **2003**, *9*, 2986−2987. (l) Tsuda, A.; Nakamura, Y.; Osuka, A. *Chem. Commun.* **2003**, *9*, 1096−1097. (m) Tsuda, A.; Osuka, A. *Science* **2001**, *293*, 79−82. (n) Tsuda, A.; Osuka, A. *Adv. Mater.* **2002**, *14*, 75−79.

(3) (a) Tsuda, A.; Nakamura, T.; Sakamoto, S.; Yamaguchi, K.; Osuka, A. *Angew. Chem., Int. Ed.* **2002**, *41*, 2817−2821. (b) Tsuda, A.; Sakamoto, S.; Yamaguchi, K.; Aida, T. *J. Am. Chem. Soc.* **2003**, *125*, 15722−15723. (c) Merlau, M. L.; Del Pilar Mejia, M.; Nguyen, S. T.; Hupp, J. T. *Angew. Chem., Int. Ed.* **2001**, *40*, 4239−4242. (d) Lensen, M. C.; Takazawa, K.; Elemans, J. A.; Jeukens, C. R.; Christianen, P. C.; Maan, J. C.; Rowan, A. E.; Nolte, R. J. *Chem. Eur. J.* **2004**, *10*, 831−839. (e) Iengo, E.; Zangrando, E.; Alessio, E. *Eur. J. Inorg. Chem.* **2003**, 2371−2384. (f) Hwang, I.-W.; Tae, K. A.; Dah, M. K.; Kim, D.; Kamada, T.; Nakamura, T.; Tsuda, A.; Osuka, A. *J. Am. Chem. Soc.* **2004**, *126*, 16187−16198. (g) Gunter, M. J. *Eur. J. Org. Chem.* **2004**, 1655−1673. (h) Felluga, F.; Tecilla, P.; Hillier, L.; Hunter, C. A.; Licinic, G.; Scrimin, P. *Chem. Commun.* **2000**, 1087−1088. (i) Campbell, K.; McDonald, R.; Branda, N. R.; Tykwinski, R. R. *Org. Lett.* **2001**, *3*, 1045−1048. (j) Balaban, T. S.; Linke-Schaetzel, M.; Bhise, A. D.; Vanthuyne, N.; Roussel, C.; Anson, C. E.; Buth, G.; Eichhofer, A.; Foster, K.; Garab, G.; Gliemann, H.; Goddard, R.; Javorfi, T.; Powell, A. K.; Rosner, H.; Schimmel, T. *Chem. Eur. J.* **2005**, *11*, 2267−2275. (k) Balaban, T. S.; Goddard, R.; Linke-Schaetzel, M.; Lehn, J. M. *J. Am. Chem. Soc.* **2003**, *125*, 4233−4239. (l) Takahashi, R.; Kobuke, Y. *J. Am. Chem. Soc.* **2003**, *125*, 2372−2373. (m) Ogawa, K.; Kobuke, Y. *Angew. Chem., Int. Ed.* **2000**, *39*, 4070−4073. (n) Ikeda, C.; Satake, A.; Kobuke, Y. *Org. Lett.* **2003**, *5*, 4935−4938. (o) Ikeda, C.; Fujiwara, E.; Satake, A.; Kobuke, Y. *Chem. Commun.* **2003**, 616−617. (p) Takahashi, R.; Kobuke, Y. *J. Org. Chem.* **2005**, *70*, 2745−2753. (q) Haycock, R. A.; Hunter, C. A.; James, D. A.; Michelsen, U.; Sutton, L. R. *Org. Lett.* **2000**, *2*, 2435−2438. (r) Hunter, C. A.; Tregonning, R. *Tetrahedron* **2002**, *58*, 691−697. (s) Hunter, C. A.; Low, C. M. R.; Packer, M. J.; Spey, S. E.; Vinter, J. G.; Vysotsky, M. O.; Zonta, C. *Angew. Chem., Int. Ed.* **2001**, *40*, 2678−2682. (t) Michelsen, U.; Hunter, C. A. *Angew. Chem., Int. Ed.* **2000**, *39*, 764−767.

(4) (a) Schneider, H.-J.; Tianjun, L.; Sirish, M.; Malinovski, V. *Tetrahedron* **2002**, *58*, 779−786. (b) Balaban, T. S.; Eichhöfer, A.; Lehn, J. M. *Eur. J. Org. Chem.* **2000**, 4047−4057.

(5) Haino, T.; Fujii, T.; Fukazawa, Y. *Tetrahedron Lett.* **2005**, *46*, 257−260.

(6) $\mathbf{7_b}$: Inouye, M.; Miyake, T.; Furusyo, M.; Nakazumi, H. *J. Am. Chem. Soc.* **1995**, *117*, 12416−12425. $\mathbf{7_c}$: Dumont, A.; Jacques, V.; Desreux, J. F. *Tetrahedron* **2000**, *56*, 2043−2052. $\mathbf{7_d}$: Pryor, K. E.; Shipps, G. W., Jr.; Skyler, D. A.; Rebek, J., Jr. *Tetrahedron* **1998**, *54*, 4107−4124. $\mathbf{7_f}$: Deeter, G. A.; Moore, J. F. *Macromolecules* **1993**, *26*, 2535−2541.

(7) Sun, Y.; Martell, A. E.; Tsutsui, M. *J. Heterocycl. Chem.* **1986**, *23*, 561−565.

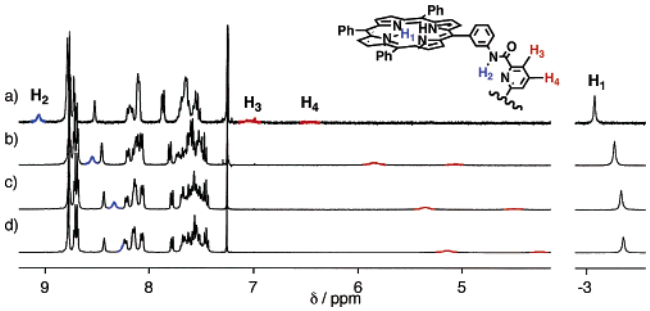

FIGURE 3. ^{1}H NMR spectra of bisporphyrin **1** in chloroform-*d* at the concentrations of (a) 1.30, (b) 5.20, (c) 10.6, and (d) 15.2 mM.

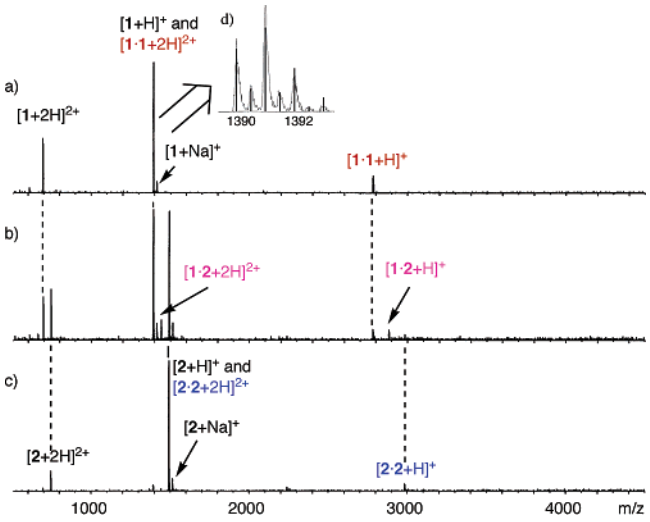

FIGURE 4. ESI mass spectra of (a) **1**, (b) a 1:1 mixture of **1** and **2**, and (c) **2** in $CHCl_3$−CH_3OH (8:2). Inset d shows the calculated (straight lines) and experimental isotopic pattern (curve). The calculated isotopic pattern is estimated on the basis of the composition of 30% [**1·1** + 2H]$^{2+}$ and 70% [**1** + H]$^+$.

confirming the elemental composition and the dimeric nature of the complex (Figure 4a,d). The ESI mass measurement of bisporphyrin **2** also indicated the formation of dimer **2·2** in the gas phase (Figure 4c). More clear evidence of the formation of the dimers can be given by the mass measurement of a 1:1 mixture of **1** and **2**. The spectrum showed the peaks *m*/*z* 2882 and 1442 belonged to dimeric species [**1·2** + H]$^+$ and [**1·2** + 2H]$^{2+}$, resulting from the heterodimerization between bisporphyrins **1** and **2** (Figure 4b).

Plotting the chemical shift changes vs the concentrations of the bisporphyrins produced the curves which nicely fit a simple dimerization model and yield formation constants K_D (Table 1). Judging from the resultant binding data for **1** and **2** vs **5** and **6**, the presence of nitrogen in the aromatic ring linking two

TABLE 1. Dimerization Constants K_D of Bisporphyrins 1−6 at 295 K

compd	solvent	K_D (M^{-1})	ΔG (kcal·mol^{-1})
1	$CDCl_3$	310 ± 20	−3.4 ± 0.1
1	toluene-d_8	5500 ± 500	−5.0 ± 0.1
2	$CDCl_3$	75 ± 1	−2.5 ± 0.1
2	toluene-d_8	830 ± 30	−3.9 ± 0.1
3	$CDCl_3$	205 ± 4	−3.1 ± 0.1
4	$CDCl_3$	121 ± 2	−2.8 ± 0.1
5	$CDCl_3$	98 ± 2	−2.7 ± 0.1
6	$CDCl_3$	15.8 ± 0.4	−1.6 ± 0.1

porphyrins plays a key role in the formation of the dimers. The substitution of the hexyloxy group on the aromatic rings reduces the stability of the dimers. Moreover, the obvious solvent effect is seen in bisporphyrins **1** and **2**; the stabilities of the dimers in toluene dramatically increased as compared with those in chloroform.

Determining the structures of the dimers in solution should be informative for understanding what drives the formation of the dimers. While the structures of the assembled dimers remain to be determined, theoretical calculations should provide helpful discussion. The molecular orbital (MO) method should be a first choice for the geometry calculation of the dimer. However, the reproduction of the precise geometries for such aromatic layered structures is a difficult issue in MO calculations; the effect of electron correlation (MP2) has to be included in the MO calculation to reproduce the layered geometries. However, dimer **1·1** is too large to be calculated in that way. The geometry calculation of dimer **1·1** was carried out by using MM3* as implemented in MacroModel V.6.5;[9] however, it resulted in the unlikely structure in which the cleft of the two porphyrin rings collapsed. For those reasons, the interporphyrin distance was constrained to be ca. 7 Å, which is based on the interaromatic distance between two quinone rings in the crystal structure of a quinone/porphyrin/quinone sandwich molecule.[10] The molecular modeling study gave rise to two plausible structures: one is structure **A**, in which the two molecules arranged in a self-complementary fashion, and the other is head-to-tail dimeric structure **B** (Figure 5).

The determination of a solution structure of a supramolecular assembly is quite a challenging issue. The complexation induced shift (CIS) changes of the protons give useful information to determine which is predominant in solution. The CIS changes for all assignable protons of the bisporphyrins were estimated by nonlinear least-squares regression analyses (Table 2). In both structures, H_3, H_4, H_{10}, and H_{11} protons experienced the large shielding effect due to the anisotropic contribution of the porphyrin rings, causing their large upfield shifts, which place them between the bisporphyrin rings.

We have developed a chemical shift simulation program,[11] which can estimate a local anisotropic shielding contribution of a porphyrin ring as well as an aromatic ring, to present the complexation induced chemical shift changes of protons along

(8) (a) Przybylski, M.; Glocker, M. O. *Angew. Chem., Int. Ed. Engl.* **1996**, *35*, 806−826. (b) Schweiger, M.; Seidel, S. R.; Schmitz, M.; Stang, P. J. *Org. Lett.* **2000**, *2*, 1255−1257. (c) Jacopozzi, P.; Dalcanale, E. *Angew. Chem., Int. Ed. Engl.* **1997**, *36*, 613−615. (d) Stang, P. J.; Cao, D. H.; Chen, K.; Gray, G. M.; Muddiman, D. C.; Smith, R. D. *J. Am. Chem. Soc.* **1997**, *119*, 5163−5168. (e) Piguet, C.; Hopfgartner, G.; Bocquet, B.; Schaad, O.; Williams, A. F. *J. Am. Chem. Soc.* **1994**, *116*, 9092−9102. (f) Bitsch, F.; Dietrich-Buchecker, C. O.; Khémiss, A.-K.; Sauvage, J.-P.; Dorsselaer, A. V. *J. Am. Chem. Soc.* **1991**, *113*, 4023−4025. (g) Vincenti, M.; Dalcanale, E.; Soncini, P.; Guglielmetti, G. *J. Am. Chem. Soc.* **1990**, *112*, 445−447. (h) Schalley, C. A.; Martín, T.; Obst, U.; Rebek, J., Jr. *J. Am. Chem. Soc.* **1999**, *121*, 2133−2138. (i) Schalley, C. A.; Castellano, R. K.; Brody, M. S.; Rudkevich, D. M.; Siuzdak, G.; Rebek, J., Jr. *J. Am. Chem. Soc.* **1999**, *121*, 4568−4579.

(9) Mohamadi, F.; Richards, N. G. J.; Guida, W. C.; Liskamp, R.; Lipton, M.; Caufield, C.; Chang, G.; Hendrickson, T.; Still, W. C. *J. Comput. Chem.* **1990**, *11*, 440−467.

(10) (a) Weiser, J.; Staab, H. A. *Angew. Chem., Int. Ed. Engl.* **1984**, *23*, 623−625. (b) Krieger, C.; Weiser, J.; Staab, H. A. *Tetrahedron Lett.* **1985**, *26*, 6055−6058. (c) Kurebayashi, H.; Haino, T.; Fukazawa, Y. *Tetrahedron Lett.* **2000**, *41*, 477−480. (d) Harmata, M. *Acc. Chem. Res.* **2004**, *37*, 862−873.

(11) Iwamoto, H.; Hori, K.; Fukazawa, Y. *Tetrahedron Lett.* **2005**, *46*, 731−734.

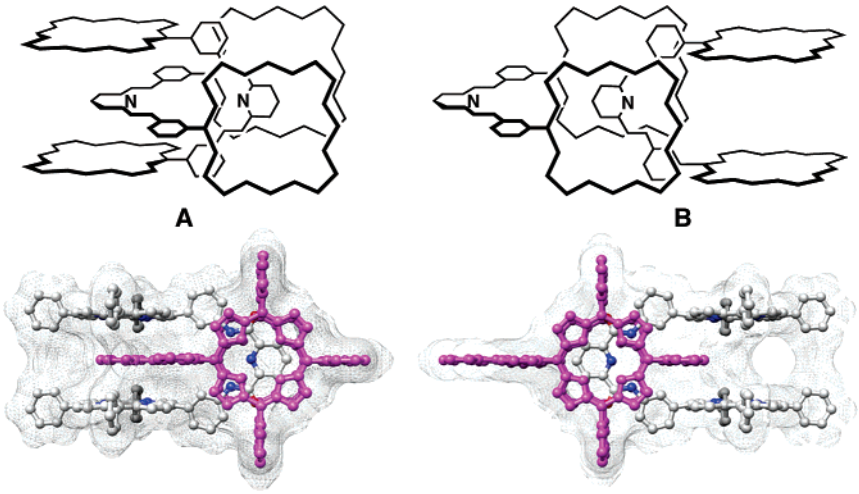

FIGURE 5. Schematic representations and calculated structures for two plausible self-assembled dimers **1·1**.

TABLE 2. The Complexation Induced Chemical Shift Changes, Δδ, of Bisporphyrins 1−6

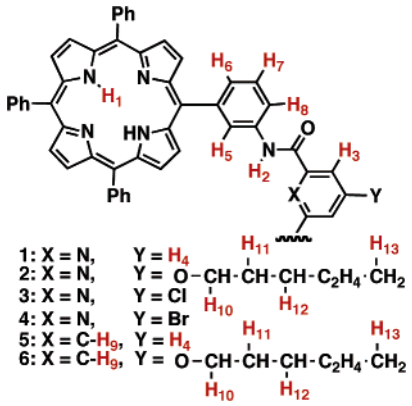

	Δδ/ppm												
compd	H_1	H_2	H_3	H_4	H_5	H_6	H_7	H_8	H_9	H_{10}	H_{11}	H_{12}	H_{13}
1	−0.80	−2.10	−5.09	−5.69	−0.28	−0.27	−0.25	−0.59					
2	−0.10	−0.66	−2.84		0.14	−0.21	−0.37	−0.64		−3.29	−2.02	−1.18	−0.07
3	−0.39	−1.51	−3.90		−0.09	−0.24	−0.34	−0.67					
4	−0.29	−1.31	−3.56		*a*	−0.23	−0.40	−0.79					
5	−0.11	−0.86	−2.98	−4.05	−0.60	−0.47	−1.13	−1.49	−0.81				
6	*a*	−0.79	−1.28		0.25	−0.50	−1.22	−1.03	−0.47	−1.84	−1.26	−1.09	−0.23

[a] Upfield shift.

the formation of an assembly having aromatic rings. Our chemical shift simulation method was applied for estimating the CIS changes of the protons of **1·1** via dimerization. The induced shift changes of protons H_2−H_8 of the linker moiety were calculated with the structures given in Figure 5.

Protons H_3 and H_4 in structure **A** show larger upfield shifts than those in **B**, and the given values for structure **A** are closer to those observed. These results conclude that dimer **1·1** predominantly adopts structure **A**. In contrast, other dimers showed smaller CIS shift changes for the pyridyl protons; the presence of the substituents at the para position of the pyridyl ring reduce the values, and isophthalamide linker is worse for complementary dimerization. These results do not allow us to rule out the presence of structure **B** in these dimers.

Structure **B** still has a binding site in one of the two bisporphyrin clefts, in which another bisporphyrin can bind to form a trimer. To confirm the presence of the trimeric structures, the electrospray mass measurements were carried out (Figure 6). The derived spectrum of bisporphyrin **5** showed several characteristic peaks, appearing at *m*/*z* 2781, 2086, and 1391, two of which were easily attributable to $[\mathbf{5{\cdot}5} + H]^+$ and $[\mathbf{5{\cdot}5} + 2H]^{2+}$; the other peak appearing at *m*/*z* 2086 was assigned to be doubly charged trimeric ion $[\mathbf{5{\cdot}5{\cdot}5} + 2H]^{2+}$. bisporphyrins **6** also showed the formation of trimer $[\mathbf{6{\cdot}6{\cdot}6} + 2H]^{2+}$ as well as dimers $[\mathbf{6{\cdot}6} + H]^+$ and $[\mathbf{6{\cdot}6} + 2H]^{2+}$ in the gas phase. A 1:1 mixture of **5** and **6** should give the four possible combinations of the trimeric structures: **5·5·5**, **5·5·6**, **5·6·6**, and **6·6·6**. The peaks of the trimeric charged species appeared as $[\mathbf{5{\cdot}5{\cdot}5} + 2H]^{2+}$, $[\mathbf{5{\cdot}5{\cdot}6} + 2H]^{2+}$, $[\mathbf{5{\cdot}6{\cdot}6} + 2H]^{2+}$, and $[\mathbf{6{\cdot}6{\cdot}6} + 2H]^{2+}$ in Figure 6b, providing a further support that bisporphyrins **5** and **6** adopt structure **B**.

For all bisporphyrins **1**−**6**, the observed *m*/*z* peaks and their relative abundances to their monomer peaks are shown in Table 4. The formation of trimers was not detected in the cases of bisporphyrins **1**−**4**, whereas the trimers of **5** and **6** possessing isophthalamide linkers stably formed in the gas phase. These

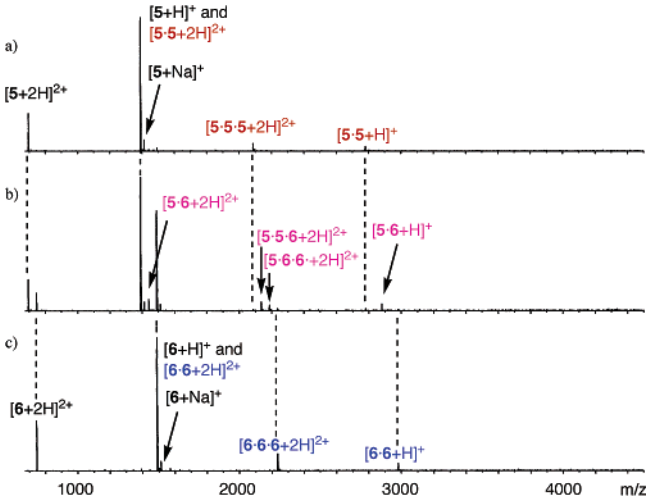

FIGURE 6. Mass spectra of (a) **5**, (b) a 1:1 mixture of **5** and **6**, and (c) **6** in $CHCl_3-CH_3OH$ (8:2).

TABLE 3. The Estimated Chemical Shift Changes via the Formation of Dimer 1·1

structure	H_2	H_3	H_4	H_5	H_6	H_7	H_8
A	−4.61	−5.46	−5.90	−0.15	0.04	0.05	−0.47
B	−2.89	−3.30	−2.94	−0.13	−0.24	0.25	−0.24
obsd	−2.10	−5.09	−5.69	−0.28	−0.27	−0.25	−0.59

results allow us to conclude that the dimers of bisporphyrins **1**−**4** possessing the pyridyl linkers mainly adopt the self-complementary structure **A** while structure **B** should be predominant in the dimers formed from **5** and **6**.

Thermodynamic Studies of the Dimerization. Van't Hoff analysis of the dimerization provides further insights into the role of the bisporphyrin cleft. The dimerization constants of the bisporphyrins were determined at four different temperatures. Van't Hoff plots gave good linear correlations, providing thermodynamic parameters for their dimerization (Figure 7, Table 5).

These association events are enthalpically favored. The porphyrin ring provides a flat and electron-rich surface, which creates $\pi-\pi$ stacking, van der Waals, and charge transfer interactions. These interactions should work within the cleft of the bisporphyrins when the flat aromatic linker moieties stay between the two porphyrin rings; thus, the main part of the enthalpic gain should come from these weak interactions working between the cleft and the linkers. The self-assembly of **2** enforces the hexyl chain into the cleft. This arrangement of the hexyl chain creates extra enthalpic benefit by means of a multitude of van der Waals contacts to the porphyrin rings, but has to pay the entropic cost due to the loss of the rotational freedom. As a result, the negative entropic contribution reduces the free energy of the assembly.

The pyridyl ring plays a key role in forming the dimerization (**1** and **2** vs **5** and **6**). The nitrogen atom of the pyridyl ring produces the hydrogen bonds to the amide N−H protons, fixing the conformational freedom around the pyridyl ring whereas such hydrogen bonds are not present in isophthalamide unit (Figure 8).[12] The well-preorganized cleft of bisporphyrins **1** and **2** brings further free energy gains for the dimerization when compared to **5** and **6**.[13]

Interestingly, the stability of the dimers **1·1** and **2·2** decreased along with the increase of the solvent polarities: the dimerization constants decrease in the order of toluene-d_8 > chloroform-d_1 > 20% methanol-d_4−chloroform-d_1. This solvent effect shows the unique solvation property of the bisporphyrins. Methanol and chloroform solvate the planar surfaces of the electron-rich porphyrin rings as well as the polar functionalities via van der Waals, CH/π, and hydrogen bonding interactions; thus the dimerization has to liberate some of the solvent molecules. Indeed, the positive value of the entropy for the dimerization in 20% methanol-d_4−chloroform-d_1 was observed, supporting that desolvation plays an important role for this association (Figure 9).[14]

Guest Binding Studies. It is known that the bisporphyrin family provides the electron-rich cleft in which electron deficient aromatic guests are accommodated in organic solvents.[15] If bisporphyrin **1** binds some aromatic guests, its self-assembly can be regulated by guest binding. Judging from the dimerization constant of **1** at 298 K in chloroform-d_1, the molar fraction of the monomer of **1** is more than 97% when its concentration is lower than 2×10^{-5} mol/L. The titration experiments of **1** with the aromatic guests were carried out in this concentration by using absorption spectra (Figure 10).

During the addition of **9**, the absorption spectra showed characteristic changes at Soret and Q-bands, and isosbestic points appeared, indicating that bisporphyrin **1** takes up electron deficient aromatic guest **9** within the cleft to form a 1:1 host−guest complex. Plotting the changes of the absorption at 434 nm vs the concentration of **9** produced a curve, nicely fit to a 1:1 host−guest model to yield the binding constant (K_a: 410 000 ± 10 000 L mol^{-1}).

The structural information of the host−guest complex was given by the ^{1}H NMR spectra. The five discrete proton resonances of guest **9** appear in the aromatic region (Figure 12a). When a stoichiometric amount of bisporphyrin **1** was added into the solution of **9**, the guest protons shifted upfield and their signals were relatively broadened due to the large difference between the chemical shifts of the bound and free guests (Figure 12b). Further addition of **1** to the solution of **9** resulted in the sharp signals with the large upfield shifts (Table 6), indicating that the guest was completely taken up within the bisporphyrin cleft in which its protons experienced the high shielding effect.

A molecular modeling study of the host−guest complexes provides further information of the molecular structure of them. A stereoplot of the calculated structure of **1·9** is shown in Figure 13. In the calculated structure, guest **9** stacks nicely between the two porphyrin rings, which rationalizes the large upfield shifts of the guest protons.

Other aromatic guests **10**−**17** were assessed in the same way. Every bound guest shows the large CIS values, indicating that the bisporphyrin takes up its guest within the cleft. Electron

(12) (a) Hunter, C. A.; Purvis, D. H. *Angew. Chem., Int. Ed. Engl.* **1992**, *31*, 792−795. (b) Hamuro, Y.; Geib, S. J.; Hamilton, A. D. *Angew. Chem., Int. Ed. Engl.* **1994**, *33*, 446−448.

(13) Cram, D. J. *Angew. Chem., Int. Ed. Engl.* **1988**, *27*, 1009−1020.

(14) Yanase, M.; Matsuoka, M.; Tatsumi, Y.; Suzuki, M.; Iwamoto, H.; Haino, T.; Fukazawa, Y. *Tetrahedron Lett.* **2000**, *41*, 493−497.

(15) (a) Sirish, M.; Chertkov, V. A.; Schneider, H. J. *Chem. Eur. J.* **2002**, *8*, 1181−1188. (b) Sun, D.; Tham, F. S.; Reed, C. A.; Chaker, L.; Boyd, P. D. *J. Am. Chem. Soc.* **2002**, *124*, 6604−6612. (c) Yagi, S.; Ezoe, M.; Yonekura, I.; Takagishi, T.; Nakazumi, H. *J. Am. Chem. Soc.* **2003**, *125*, 4068−4069. (d) Uno, H.; Masumoto, A.; Ono, N. *J. Am. Chem. Soc.* **2003**, *125*, 12082−12083.

TABLE 4. Electrospray Mass Measurements for Bisporphyrins 1−6

		obs. mass			% abundance		
compd	MF	monomer	dimer	trimer	monomer	dimer	trimer
1	$C_{95}H_{63}N_{11}O_2$	1392	2783		100	13	0
1 + **2**	$C_{196}H_{138}N_{22}O_5$		2882		100	8	0
2	$C_{101}H_{75}N_{11}O_3$	1492	2983		100	6	0
3	$C_{95}H_{62}N_{11}O_2Cl$	1426	2851		100	17	0
4	$C_{95}H_{62}N_{11}O_2Br$	1471	2941		100	14	0
5	$C_{96}H_{64}N_{10}O_2$	1391	2781	2086	100	6	7
5 + **6**	$C_{198}H_{140}N_{20}O_5$		2880	2136, 2186	100	5	7, 5
6	$C_{102}H_{76}N_{10}O_3$	1491	2981	2235	100	6	13

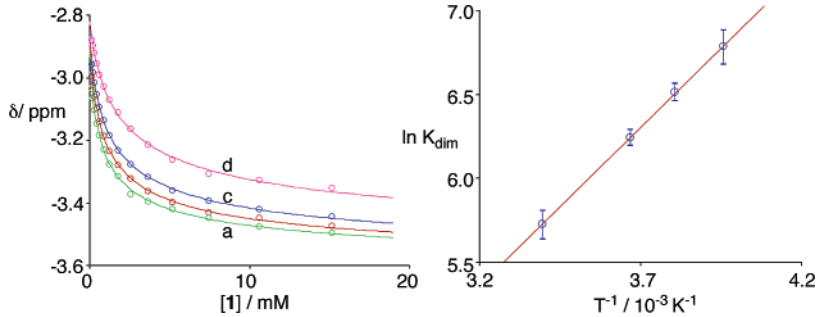

FIGURE 7. The titration curves for **1** in chloroform-d_1 at (a) 253, (b) 263, (c) 273, and (d) 295 K, and its Van't Hoff plot.

TABLE 5. Thermodynamic Parameters for the Dimerization of Bisporphyrins 1−6

compd	solvent	ΔH (kcal mol^{-1})	ΔS (cal mol^{-1} K^{-1})	ΔG (kcal mol^{-1})
1	toluene-d_8	−7.1 ± 0.2	−5.8 ± 0.5	−5.0 ± 0.1
1	$CDCl_3$	−3.8 ± 0.1	−1.7 ± 0.2	−3.4 ± 0.1
1	20% CD_3OD−$CDCl_3$	−1.3 ± 0.1	3.8 ± 0.5	−2.4 ± 0.1
2	toluene-d_8	−7.2 ± 0.1	−10.6 ± 0.1	−3.9 ± 0.1
2	$CDCl_3$	−5.1 ± 0.1	−9.1 ± 0.5	−2.5 ± 0.1
3	$CDCl_3$	−4.7 ± 0.1	−5.3 ± 0.2	−3.1 ± 0.1
4	$CDCl_3$	−4.0 ± 0.3	−4.1 ± 1.0	−2.8 ± 0.1
5	$CDCl_3$	−3.3 ± 0.1	−2.0 ± 0.4	−2.7 ± 0.1
6	$CDCl_3$	−4.4 ± 0.2	−9.3 ± 0.9	−1.6 ± 0.1

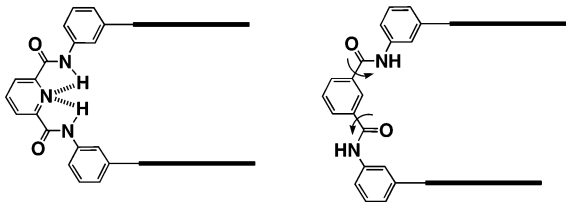

FIGURE 8. Preferential conformations of bisporphyrins.

deficient planar aromatic guests **9**−**11** possessing the wide contact surfaces for the bisporphyrin resulted in distinctively strong binding affinities. The notable trends for the stability of the host−guest complexes are seen in the series of benzene derivatives **12**−**14** and **15**−**17**; the more electron deficient benzene ring works rather well as a guest compared to the others (**12** and **15** vs **13**, **14** ,and **16**, **17**). On the basis of the binding data (Table 6), it is concluded that the $\pi-\pi$ stacking and charge transfer interactions between the bound guest and the two porphyrin rings mainly drive these associations.

The association constant of aromatic guest **9** to the bisporphyrin is more than 1000 times as large as its dimerization constant. The association of the dimer can thus be regulated by the addition of the guest. Decomplexation of bisporphyrin dimer **1·1** was carried out by the addition of **9** in chloroform-d_1.

The molar fraction of dimer **1·1** is about 60% at the concentration of 7.0 mmol L^{-1} in chloroform-d_1. When a small amount of **9** was added into the solution of the dimer, the sharp signals of the bound guest appeared in the range between 4 and 7 ppm whereas the signals of the aromatic region were broadened due to the equilibrium among **1·1**, **1**, **9**, and **1·9** (Figure 14b,c). Further addition of **9** resulted in the relatively sharp and well-split signals in the aromatic regions. The

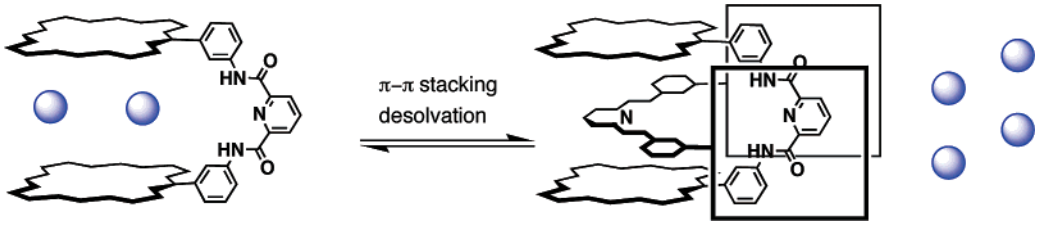

FIGURE 9. Schematic representation of the desolvation via self-assembly.

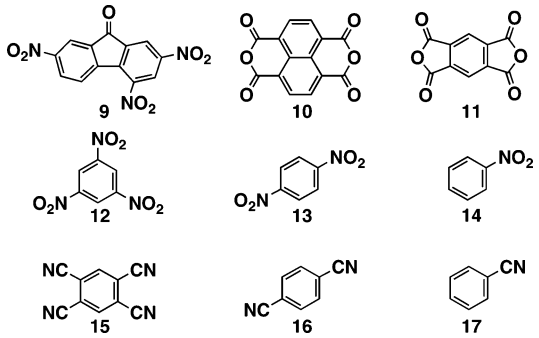

FIGURE 10. Aromatic guests.

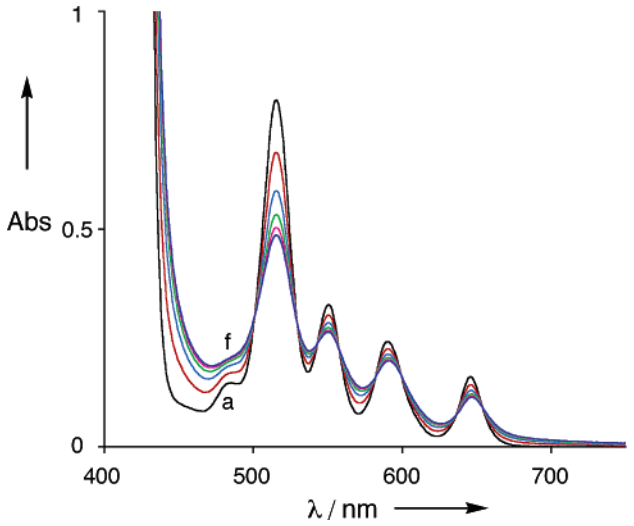

FIGURE 11. Absorption spectra of **1** (2.0×10^{-5} mol L^{-1}) in the presence of **9** at 298 K in chloroform. The concentrations of **9** are from the bottom (a) 0.0, (b) 0.8×10^{-5}, (c) 1.6×10^{-5}, (d) 2.4×10^{-5}, (e) 3.2×10^{-5}, and (f) 40.0×10^{-5} mol L^{-1}.

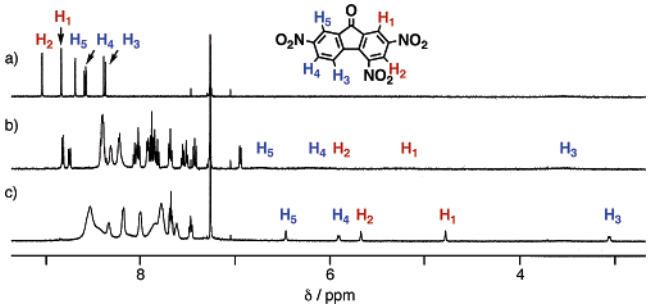

FIGURE 12. ^{1}H NMR spectra of **9** (1.0×10^{-3} mol L^{-1}) in the presence of **1** at 298 K in chloroform-d_1. The concentrations of **1** are (a) 0.0, (b) 1.0×10^{-3}, and (c) 2.0×10^{-3} mol L^{-1}.

chemical shifts of H_7 and H_8 reached 8.82 and 8.37 ppm, which are common chemical shifts observed for pyridyl protons. These results indicate that dimer **1·1** was completely dissociated by the complexation of **9** to form monomeric bisporphyrin complex **1·9**.

Conclusion

Bisporphyrins **1**−**6** assemble to form the dimers and the trimers. Our chemical shift simulation predicted the complexation-induced shifts for dimer **1·1**. Judging from a comparison between the predicted and observed values, the dimer adopts self-complementary structure **A**. On the basis of the thermodynamic studies for the self-assemblies, it is clear that not only many subtle interactions such as van der Waals, CH/π, and $\pi-\pi$ stacking interaction but also the desolvation regulate the self-assembling phenomena. The bisporphyrin can work as a good host for flat aromatic guests. Electron deficient guests bound between the bisporphyrin cleft via charge transfer as well as van der Waals, CH/π, and $\pi-\pi$ stacking interactions. During the studies, we found very good aromatic guests **9**−**11**, which showed extremely strong binding affinities for **1**. The decomplexation of **1·1** was achieved by addition of **9** to form **1·9**. The self-assembling of **1** can be regulated by the guest complexation, giving a wide range of possible scope for the application including molecular devices and information storage.

TABLE 6. Binding Constants of 1 with Aromatic Guests 9−17 at 298 K in Chloroform and Their Complexation Induced Shifts (Δδ)

guest	K_a (M^{-1})	ΔG (kcal·mol^{-1})	CIS ($\delta\delta$)/ppm
9	410 000 ± 10 000	−7.65 ± 0.01	H1: −4.02, H2: −3.33, H3: −5.27,H4: −2.65,
10	170 000 ± 30 000	−7.1 ± 0.1	H5: −2.20
11	121 000 ± 6000	−6.93 ± 0.02	−7.56
12	8500 ± 200	−5.36 ± 0.01	−6.78
13	290 ± 7	−3.36 ± 0.01	−2.86
14	N.B.		
15	8700 ± 600	−5.37 ± 0.04	−6.87
16	N.B.		
17	N.B.		

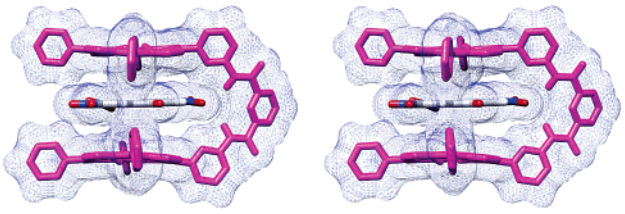

FIGURE 13. Stereoplot of the calculated structure for the host−guest complex of **1** with **9**.

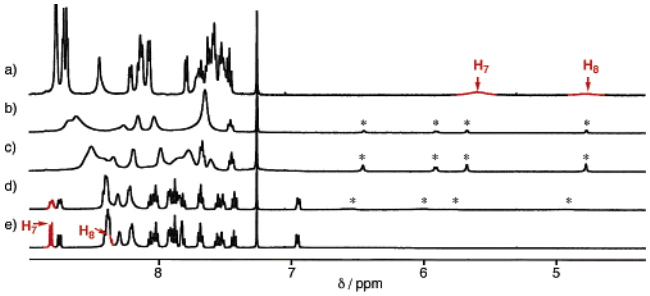

FIGURE 14. ^{1}H NMR spectra of **1** (7.0×10^{-3} mol L^{-1}) in the presence of **9** at 298 K in chloroform-d_1. The concentrations of **9** are (a) 0.0, (b) 2.8×10^{-3}, (c) 4.9×10^{-3}, (d) 7.7×10^{-3}, and (e) 9.8×10^{-3} mol L^{-1}. An asterisk denotes bound guest signals.

Experimental Section

***N,N′*-Bis[3-(10,15,20-triphenyl-21*H*,23*H*-porphin-5-yl)phenyl]-2,6-pyridinedicarboxamide (1).** To a solution of **8** (85.0 mg, 0.135 mmol), a catalytic amount of 4-(dimethylamino)pyridine, and triethylamine (0.10 mL, 0.70 mmol) in THF (6 mL) was added a solution of $\mathbf{7_a}$ (12.0 mg, 0.061 mmol) in THF (2 mL) at 0 °C. After being stirred overnight, the reaction mixture was diluted with methylene chloride. The organic layer was washed with aqueous

sodium bicarbonate, dried over sodium sulfate, and concentrated in vacuo. The residue was purified by column chromatography on silica gel (80% CH_2Cl_2−hexane) to give purple solid **1** (26.0 mg, 31%). ^{1}H NMR (500 MHz, 10 mM, $CDCl_3$) δ 8.78 (m, 8H), 8.73 (d, 4H, J = 4.9 Hz), 8.70 (d, 4H, J = 4.9 Hz), 8.45 (s, 2H), 8.36 (br s, 2H), 8.22 (d, 2H, J = 7.3 Hz), 8.16−8.13 (m, 6H), 8.07 (d, 4H, J = 7.3 Hz), 7.79 (d, 2H, J = 8.0 Hz), 7.71 (d, 2H, J = 8.0 Hz), 7.70−7.48 (m, 18H), 7.47 (t, 2H, J = 8.0 Hz), 5.43 (br s, 2H), 4.59 (br s, 1H), −3.32 (br s, 4H) ppm; ^{13}C NMR (125 MHz, 10 mM, $CDCl_3$) δ 159.4, 145.4, 142.8, 142.1, 142.0, 135.6, 135.5, 134.6, 134.5, 131.2, 127.6, 127.0, 126.6, 125.7, 122.2, 120.3, 120.0, 119.0, 118.9 ppm; IR (KBr) 3375, 3314, 1689, 1532 cm^{-1}; UV−vis ($CHCl_3$) λ_{max} (ϵ) 418.5 (7.66×10^5), 515.5 (3.33×10^4), 550.5 (1.33×10^4), 590.0 (9.65×10^3), 645.5 (5.96×10^3) nm; ESI-MS m/z 1392.0 [**1** + H]$^+$, 2782.5 [**1·1** + H]$^+$; FAB-MS m/z 1391 [**1** + H]$^+$; HRMS (FAB$^+$) m/z calcd for $C_{95}H_{64}N_{11}O_2$ 1390.5244, found 1390.5210 [M + H]$^+$. Anal. Calcd for $C_{95}H_{63}N_{11}O_2{\cdot}2.5H_2O$: C 79.47, H 4.78, N 10.73. Found: C 79.39, H 4.54, N 10.73.

4-(Hexyloxy)-*N*,*N*′-bis[3-(10,15,20-triphenyl-21*H*,23*H*-porphin-5-yl)phenyl]-2,6-pyridinedicarboxamide (2). To a solution of **8** (21.0 mg, 0.033 mmol), a catalytic amount of 4-(dimethylamino)-pyridine, and triethylamine (0.021 mL, 0.15 mmol) in THF (1 mL) was added a solution of **7$_b$** (5.0 mg, 0.016 mmol) in THF (1 mL) at 0 °C. After being stirred overnight, the reaction mixture was diluted with methylene chloride. The organic layer was washed with aqueous sodium bicarbonate, dried over sodium sulfate, and concentrated in vacuo. The residue was purified by column chromatography on silica gel (80% CH_2Cl_2−hexane) to give purple solid **2** (17.0 mg, 41%). ^{1}H NMR (500 MHz, 10 mM, $CDCl_3$) δ 9.51 (s, 2H), 8.85 (d, 4H, J = 4.6 Hz), 8.83 (d, 4H, J = 4.6 Hz), 8.78 (d, 4H, J = 4.6 Hz), 8.74 (d, 4H, J = 4.6 Hz), 8.66 (s, 2H), 8.25 (d, 2H, J = 6.7 Hz), 8.17−8.14 (m, 10H), 7.85 (d, 2H, J = 7.6 Hz), 7.79 (d, 2H, J = 7.6 Hz), 7.72−7.54 (m, 18H), 7.45 (t, 2H, J = 7.6 Hz), 6.87 (br s, 2H), 2.86 (br s, 2H), 1.14 (m, 2H), 1.04−0.98 (m, 4H), 0.91 (m, 2H), 0.80 (t, 3H, J = 7.3 Hz), −2.88 (br s, 4H) ppm; ^{13}C NMR (125 MHz, 10 mM, $CDCl_3$) δ 167.0, 161.0, 149.8, 143.0, 142.2, 142.0, 135.6, 134.6, 134.5, 131.2, 127.7, 127.6, 127.1, 126.64, 126.57, 126.4, 120.25, 120.16, 119.5, 119.0, 110.7, 68.3, 31.2, 28.0, 25.0, 22.3, 13.9 ppm; IR (KBr) 3373, 3314, 1691, 1530 cm^{-1}; UV−vis ($CHCl_3$) λ_{max} (ϵ) 418.5 (7.39×10^5), 516.0 (3.37×10^4), 551.0 (1.47×10^4), 590.0 (1.07×10^4), 646.0 (6.24×10^3) nm; ESI-MS m/z 1491.9 [**2** + H]$^+$, 2982.5 [**2·2** + H]$^+$; FAB-MS m/z 1491 [**2** + H]$^+$; HR MS (FAB$^+$) m/z calcd for $C_{101}H_{76}N_{11}O_3$ 1490.6133, found 1490.6161 [M + H]$^+$. Anal. Calcd for $C_{101}H_{75}N_{11}O_3{\cdot}3PrOH{\cdot}CH_3CN$: C 78.57, H 6.02, N 9.82. Found: C 78.47, H 6.31, N 9.86.

4-(Chloro)-*N*,*N*′-bis[3-(10,15,20-triphenyl-21*H*,23*H*-porphin-5-yl)phenyl]-2,6-pyridinedicarboxamide (3). To a solution of **8** (370.0 mg, 0.59 mmol), a catalytic amount of 4-(dimethylamino)-pyridine, and pyridine (0.5 mL, 6.18 mmol) in THF (10 mL) was added a solution of **7$_c$** (54.0 mg, 0.23 mmol) in THF (3 mL) at 0 °C. After being stirred overnight, the reaction mixture was diluted with methylenechloride. The organic layer was washed with aqueous sodium bicarbonate, dried over sodium sulfate, and concentrated in vacuo. The residue was purified by column chromatography on silica gel (80% CH_2Cl_2−hexane) to give purple solid **3** (95.0 mg, 29%). ^{1}H NMR (500 MHz, 10 mM, $CDCl_3$) δ 8.83 (d, 4H, J = 4.6 Hz), 8.80 (d, 4H, J = 4.6 Hz), 8.72 (m, 8H), 8.66 (br s, 2H), 8.52 (s, 2H), 8.24 (d, 2H, J = 6.8 Hz), 8.19−8.18 (m, 6H), 8.08 (d, 4H, J = 7.0 Hz), 7.83 (d, 2H, J = 7.4 Hz), 7.70−7.51 (m, 20H), 7.42 (t, 2H, J = 7.6 Hz), 6.13 (br s, 2H), −3.08 (s, 4H) ppm; ^{13}C NMR (75 MHz, 10 mM, $CDCl_3$) δ 158.8, 142.9, 142.1, 142.0, 135.2, 134.6, 134.4, 131.3, 127.6, 127.1, 126.6, 126.0, 123.3, 120.4, 120.1, 119.3, 118.7 ppm; IR (KBr) 3389, 3314, 1692, 1535 cm^{-1}; UV−vis ($CHCl_3$) λ_{max} (ϵ) 418.0 (8.37×10^5), 515.0 (3.72×10^4), 550.0 (1.50×10^4), 590.0 (1.09×10^4), 646.0 (7.52×10^3) nm; FAB-MS m/z 1425 [**4** + H]$^+$; ESI-MS m/z 1426.4 [**4** + H]$^+$, 2851.1 [**4·4** + H]$^+$; HR MS (FAB$^+$) m/z calcd for $C_{95}H_{63}{}^{37}ClN_{11}O_2$ 1426.4825, found 1426.4845 [M + H]$^+$.

4-(Bromo)-*N*,*N*′-bis[3-(10,15,20-triphenyl-21*H*,23*H*-porphin-5-yl)phenyl]-2,6-pyridinedicarboxamide (4). To a solution of **8** (228.0 mg, 0.360 mmol), a catalytic amount of 4-(dimethylamino)-pyridine, and pyridine (0.5 mL, 6.18 mmol) in THF (10 mL) was added a solution of **7$_d$** (49.0 mg, 0.17 mmol) in THF (3 mL) at 0 °C. After being stirred overnight, the reaction mixture was diluted with methylene chloride. The organic layer was washed with aqueous sodium bicarbonate, dried over sodium sulfate, and concentrated in vacuo. The residue was purified by column chromatography on silica gel (80% CH_2Cl_2−hexane) to give purple solid **4** (107.0 mg, 43%). ^{1}H NMR (500 MHz, 10 mM, $CDCl_3$) δ 8.87 (br s, 2), 8.84 (d, 4H, J = 4.6 Hz), 8.81 (d, 4H, J = 4.6 Hz), 8.74−8.73 (m, 8H), 8.56 (s, 2H), 8.25(d, 2H, J = 7.4 Hz), 8.18 (d, 6H, J = 7.4 Hz), 8.10 (d, 4H, J = 7.4 Hz), 7.84 (d, 2H, J = 7.4 Hz), 7.72−7.49 (m, 20H), 7.40 (t, 2H, J = 7.4 Hz), 6.77 (br s, 2H), −3.00 (br s, 4H) ppm; ^{13}C NMR (125 MHz, 10 mM, $CDCl_3$) δ 159.1, 147.7, 142.9, 142.1, 142.0, 135.1, 134.6, 131.3, 127.6, 127.1, 126.6, 126.2, 120.4, 120.1, 119.4, 118.7 ppm; IR (KBr) 3407, 3319, 1685, 1531 cm^{-1}; UV−vis ($CHCl_3$) λ_{max} (ϵ) 418.0 (8.27×10^5), 515.0 (3.68×10^4), 550.0 (1.53×10^4), 591.0 (1.19×10^4), 646.0 (6.90×10^3) nm; FAB-MS m/z 1470 [**5** + H]$^+$; ESI-MS m/z 1471.2 [**5** + H]$^+$, 2940.7 [**5·5** + H]$^+$; HR MS (FAB$^+$) m/z calcd for $C_{95}H_{63}{}^{81}ClN_{11}O_2$ 1470.4329, found 1470.4327 [M + H]$^+$.

***N*,*N*′-Bis[3-(10,15,20-triphenyl-21*H*,23*H*-porphin-5-yl)phenyl]-1,3-benzenedicarboxamide (5).** To a solution of **8** (130.0 mg, 0.210 mmol), a catalytic amount of 4-(dimethylamino)pyridine, and pyridine (0.5 mL, 6.18 mmol) in THF (5 mL) was added a solution of **7$_e$** (19.0 mg, 0.10 mmol) in THF (1 mL) at 0 °C. After being stirred overnight, the reaction mixture was diluted with methylene chloride. The organic layer was washed with aqueous sodium bicarbonate, dried over sodium sulfate, and concentrated in vacuo. The residue was purified by column chromatography on silica gel (80% CH_2Cl_2−hexane) to give purple solid **5** (45.0 mg, 32%). ^{1}H NMR (500 MHz, 10 mM, $CDCl_3$) δ 8.88 (d, 4H, J = 4.6 Hz), 8.80 (d, 4H, J = 4.6 Hz), 8.69 (d, 4H, J = 4.6 Hz), 8.62 (d, 4H, J = 4.6 Hz), 8.25 (d, 2H, J = 6.4 Hz), 8.21 (d, 2H, J = 6.4 Hz), 8.12 (s, 1H), 8.10 (d, 4H, J = 6.7 Hz), 8.04 (s, 2H), 7.81−7.74 (m, 14H), 7.62 (t, 4H, J = 7.3 Hz), 7.54 (t, 4H, J = 7.3 Hz), 7.44 (d, 2H, J = 7.6 Hz), 7.23−7.18 (m, 6H), 6.59 (br s, 2H), 5.55 (br s, 1H), −2.87 (br s, 4H) ppm; ^{13}C NMR (125 MHz, 10 mM, $CDCl_3$) δ 164.6, 142.7, 142.1, 141.8, 135.8, 134.6, 134.5, 134.4, 134.2, 134.1, 130.9, 129.0, 127.9, 127.8, 127.5, 127.1, 126.71, 126.67, 126.6, 126.53, 126.45, 124.6, 120.4, 120.1, 119.6, 118.9 ppm; IR (KBr) 3419, 3315, 1675, 1540 cm^{-1}; UV−vis ($CHCl_3$) 418.5, 515.5, 551.0, 590.0, 646.0 nm; ESI-MS m/z 1390.8 [**6** + H]$^+$, 2780.5 [**6·6** + H]$^+$; FAB-MS m/z 1390 [**6** + H]$^+$; HR MS (FAB$^+$) m/z calcd for $C_{96}H_{65}N_{10}O_2$ 1389.5292, found 1389.5302 [M + H]$^+$. Anal. Calcd for $C_{96}H_{64}N_{10}O_2{\cdot}2EtOH$: C 81.06, H 5.17, N 9.45. Found: C 81.24, H 5.18, N 9.72.

5-(Hexyloxy)-*N*,*N*′-bis[3-(10,15,20-triphenyl-21*H*,23*H*-porphin-5-yl)phenyl]-1,3-benzenedicarboxamide (6). To a solution of **8** (250.0 mg, 0.400 mmol), a catalytic amount of 4-(dimethylamino)-pyridine, and pyridine (0.5 mL, 6.18 mmol) in THF (4 mL) was added a solution of **7$_f$** (55.0 mg, 0.18 mmol) in THF (1 mL) at 0 °C. After being stirred overnight, the reaction mixture was diluted with methylene chloride. The organic layer was washed with aqueous sodium bicarbonate, dried over sodium sulfate, and concentrated in vacuo. The residue was purified by column chromatography on silica gel (80% CH_2Cl_2−hexane) to give purple solid **6** (66.0 mg, 25%). ^{1}H NMR (500 MHz, 10 mM, $CDCl_3$) δ 8.85−8.83 (m, 12H), 8.79 (d, 4H, J = 4.3 Hz), 8.39 (s, 2H), 8.30 (s, 2H), 8.22 (d, 4H, J = 6.7 Hz), 8.18 (d, 4H, J = 6.4 Hz), 8.13 (d, 2H, J = 6.4 Hz), 7.96 (d, 2H, J = 7.4 Hz), 7.92 (d, 2H, J = 7.4 Hz), 7.79−7.56 (m, 18H), 7.51 (t, 2H, J = 7.4 Hz), 7.38 (s, 2H), 3.70 (br s, 2H), 1.29−1.16 (m, 6H), 0.79 (t, 3H, J = 7.0 Hz) ppm; ^{13}C NMR (125 MHz, 10 mM, $CDCl_3$) δ 165.0, 159.7, 143.0, 142.1, 142.0, 136.5, 136.1, 134.5, 131.4, 131.3, 127.7, 127.6,

127.3, 126.7, 126.6, 120.3, 120.2, 119.6, 119.0, 116.9, 116.8, 116.5, 68.5, 31.4, 28.8, 25.4, 22.4, 13.9 ppm; IR (KBr) 3412, 3315, 1684, 1528 cm^{-1}; UV−vis ($CHCl_3$) λ_{max} (ϵ) 418.0 (8.43×10^5), 515.0 (3.55×10^4), 550.0 (1.40×10^4), 590.0 (1.00×10^4), 645.0 (6.37×10^3) nm; ESI-MS *m*/*z* 1490.9 [**7** + H]$^+$, 2980.6 [**7**·**7** + H]$^+$; FAB-MS *m*/*z* 1490 [**7** + H]$^+$; HR MS (FAB$^+$) *m*/*z* calcd for $C_{102}H_{77}N_{10}O_3$ 1489.6180, found 1489.6178 [M + H]$^+$. Anal. Calcd for $C_{102}H_{76}N_{10}O_3$·1.67EtOH: C 80.75, H 5.54, N 8.94. Found: C 80.51, H 5.81, N 9.16.

Acknowledgment. We thank Professor Misako Aida for helpful discussions regarding the molecular modeling.

JO052224B